International Journal of Scientific Research and Engineering Development-– Volume 9 Issue 4, July – August 2026
Available at www.ijsred.com

RESEARCH ARTICLE OPEN ACCESS

Phase Evolution & Dielectric Properties of $ZnNb_2O_6$ Columbite Phase

Harshit Yadav[1], S.K. Chaudhary[2], Praveen Kumar[2]
[1]Research Scholar, Deparartment of Physics, P.K. University,Shivpuri (M.P.)
[2]Assistant Professor, Deparartment of Physics, P.K. University, Shivpuri (M.P.)

Abstract:
Zinc oxide (ZnO) nanoparticles have emerged as promising multifunctional materials due to their unique structural, optical, and magnetic properties. In this study, ZnO nanoparticles were synthesized using a chemical route and systematically characterized to investigate phase formation and magnetic behavior. X-ray diffraction (XRD) confirmed the formation of a single-phase hexagonal wurtzite structure with high crystallinity. The average crystallite size was estimated using the Scherrer equation and found to be in the nanometer range. Magnetic measurements using a vibrating sample magnetometer (VSM) revealed weak room-temperature ferromagnetism, attributed to intrinsic defects such as oxygen vacancies and zinc interstitials. The results establish a strong correlation between structural defects and magnetic properties, highlighting the potential of ZnO nanoparticles in spintronic applications.

Keywords: ***ZnO nanoparticles, XRD, phase analysis, ferromagnetism, defects, VSM***

1. Introduction

Nanostructured materials have emerged as a central focus of modern materials science due to their size-dependent physical and chemical properties, which differ significantly from their bulk counterparts. When the particle size is reduced to the nanometer scale (1–100 nm), phenomena such as quantum confinement, increased surface-to-volume ratio, and enhanced defect density lead to remarkable changes in optical, electrical, and magnetic behavior. Among various metal oxide semiconductors, zinc oxide (ZnO) has attracted extensive attention owing to its multifunctional characteristics and technological relevance.

ZnO is a II–VI semiconductor with a wide direct bandgap of approximately 3.37 eV and a large exciton binding energy of about 60 meV at room temperature. These properties make it highly suitable for applications in optoelectronic devices such as light-emitting diodes, laser diodes, photodetectors, and transparent conducting electrodes. Additionally, ZnO exhibits excellent chemical stability, non-toxicity, and biocompatibility, which further extend its applications to sensors, photocatalysis, and biomedical devices.

Structurally, ZnO predominantly crystallizes in the hexagonal wurtzite phase under ambient conditions, which is thermodynamically stable. The wurtzite structure is characterized by tetrahedral coordination of Zn^{2+} and O^{2-} ions and exhibits non-centrosymmetric properties, giving rise to piezoelectric and pyroelectric behavior. At the nanoscale, however, structural properties such as lattice parameters, crystallinity, and phase stability can be significantly influenced by synthesis conditions, particle size, and surface energy.

In recent years, considerable interest has been directed toward the magnetic properties of ZnO nanoparticles. Bulk ZnO is intrinsically diamagnetic; however, several experimental reports have demonstrated unexpected room-temperature ferromagnetism (RTFM) in undoped ZnO nanostructures. This observation has opened new avenues for the development of dilute magnetic semiconductors and spintronic devices, where both charge and spin of electrons are utilized for information processing.

The origin of ferromagnetism in ZnO nanoparticles remains a subject of ongoing debate. Unlike conventional magnetic materials, where magnetism arises from partially filled d-orbitals of transition metals, ZnO exhibits so-called d^0 *ferromagnetism*,

where magnetic ordering is induced without magnetic ion doping. Various mechanisms have been proposed to explain this phenomenon, among which defect-induced magnetism is the most widely accepted. Intrinsic defects such as oxygen vacancies (V_O), zinc interstitials (Zn_i), and zinc vacancies (V_Zn) are believed to introduce localized magnetic moments within the lattice. These localized moments can interact through exchange mechanisms, such as the bound magnetic polaron (BMP) model, leading to long-range ferromagnetic ordering.

Despite numerous studies, there are still significant inconsistencies in the reported magnetic behavior of ZnO nanoparticles. Some researchers attribute the observed ferromagnetism to intrinsic defects, while others suggest that it may arise from extrinsic factors such as contamination or secondary phases. Furthermore, the relationship between phase purity, crystallite size, defect concentration, and magnetic properties has not been fully established.

Phase evaluation plays a crucial role in understanding these properties, as even minor structural deviations or impurity phases can significantly influence magnetic behavior. X-ray diffraction (XRD) is one of the most reliable techniques for determining crystal structure, phase purity, lattice parameters, and crystallite size. A systematic analysis of XRD patterns allows for the identification of structural defects and microstrain, which are directly linked to magnetic properties.

In this context, the present study aims to provide a comprehensive investigation of the phase formation and magnetic properties of ZnO nanoparticles synthesized via a chemical route. Special emphasis is placed on correlating structural parameters obtained from XRD analysis with magnetic characteristics measured using a vibrating sample magnetometer (VSM). By establishing a clear relationship between defects and magnetism, this work seeks to contribute to the fundamental understanding of defect-induced ferromagnetism in oxide nanomaterials.

The specific objectives of this study are as follows: (i) to synthesize ZnO nanoparticles with controlled structural properties, (ii) to perform detailed phase evaluation using XRD analysis, (iii) to estimate crystallite size and lattice strain, (iv) to investigate magnetic properties at room temperature, and (v) to establish a correlation between structural defects and magnetic behavior. The findings of this study are expected to provide valuable insights for tailoring ZnO-based materials for advanced applications in spintronics and multifunctional devices.

2. EXPERIMENTAL DETAILS

A. Materials

All chemicals used in this study were of analytical grade and used without further purification. Zinc acetate dihydrate (Zn(CH3COO)2·2H2O)(Zn($CH_3COO)_2 \cdot 2H_2O$)(Zn(CH 3COO)2·2H2O) was used as the zinc precursor, while sodium hydroxide (NaOH) served as the precipitating agent. Absolute ethanol (C_2H_5OH) was used as the solvent, and deionized water was employed throughout the experiment to avoid contamination. All glassware was cleaned thoroughly and dried prior to use to ensure experimental consistency.

B. Synthesis of ZnO Nanoparticles

ZnO nanoparticles were synthesized using a modified sol–gel method due to its advantages of simplicity, cost-effectiveness, and good control over particle size and homogeneity.

Initially, 0.1 M zinc acetate dihydrate was dissolved in 100 mL of ethanol under continuous magnetic stirring at room temperature to obtain a clear and homogeneous solution. The solution was stirred for approximately 30 minutes to ensure complete dissolution of the precursor. In a separate beaker, 0.2 M NaOH solution was prepared using deionized water. This solution was then added dropwise to the zinc acetate solution under vigorous stirring to maintain a controlled reaction environment. The pH of the solution was maintained in the range of 10–12, which is favorable for the formation of ZnO nanoparticles.

The reaction mixture was continuously stirred for 3–4 hours, resulting in the formation of a white colloidal sol. The sol was then aged at room temperature for 24 hours to promote nucleation and growth of nanoparticles.

Following aging, the precipitate was separated by centrifugation at 5000 rpm for 10 minutes and washed multiple times with ethanol and deionized water to remove residual impurities and unreacted precursors.

The cleaned precipitate was then dried in a hot air oven at 80°C for 12 hours.
The dried powder was calcined in a muffle furnace at different temperatures (400°C, 500°C, and 600°C) for 3 hours to improve crystallinity and remove any remaining organic residues. The heating rate was maintained at 5°C/min to ensure uniform thermal treatment.

C. Structural Characterization

1) X-ray Diffraction (XRD)

Phase identification and crystallographic analysis of the synthesized ZnO nanoparticles were carried out using an X-ray diffractometer equipped with Cu-Kα radiation (λ = 1.5406 Å). The diffraction patterns were recorded over a 2θ range of 20° to 80° with a step size of 0.02° and a scanning rate of 2°/min.
The obtained diffraction peaks were indexed using standard JCPDS data to confirm the formation of the hexagonal wurtzite structure. The average crystallite size (D) was calculated using the Debye–Scherrer equation:

$$D=0.9\lambda/ \beta\cos\theta$$

where λ is the wavelength of X-ray radiation, β is the full width at half maximum (FWHM) of the diffraction peak, and θ is the Bragg angle.
In addition to crystallite size, lattice parameters (a and c), microstrain (ε), and dislocation density (δ) were also evaluated using standard relations:
ε=β4tan θ\varepsilon = \frac{\beta}{4 \tan \theta}ε=4tanθβ δ=1D2\delta = \frac{1}{D^2}δ=D21

D. Morphological Characterization

1) Scanning Electron Microscopy (SEM)

Surface morphology and particle agglomeration were analyzed using scanning electron microscopy. The samples were coated with a thin layer of gold to improve conductivity before imaging. SEM micrographs provided information regarding particle shape, size distribution, and surface texture.

2) Transmission Electron Microscopy (TEM)

TEM analysis was carried out to obtain detailed information on particle size and crystallinity. A small amount of ZnO powder was ultrasonically dispersed in ethanol, and a drop of the suspension was placed on a carbon-coated copper grid. High-resolution TEM images were used to observe lattice fringes and confirm the crystalline nature of the nanoparticles.

E. Magnetic Characterization

Magnetic measurements were performed using a vibrating sample magnetometer (VSM) at room temperature. The magnetization (M) as a function of applied magnetic field (H) was recorded in the range of −10 kOe to +10 kOe.
From the obtained hysteresis loops, key magnetic parameters such as:

- Saturation magnetization (Ms)
- Coercivity (Hc)
- Remanent magnetization (Mr)

were determined. These parameters were used to evaluate the magnetic behavior of ZnO nanoparticles and to identify the presence of ferromagnetic ordering.

3. RESULTS AND DISCUSSION

A. Phase Evaluation and Structural Analysis (XRD)

The X-ray diffraction (XRD) patterns of the synthesized ZnO nanoparticles calcined at different temperatures (400°C–600°C) confirm the formation of a crystalline structure. All observed diffraction peaks can be indexed to the hexagonal wurtzite phase of ZnO, indicating successful synthesis without any detectable secondary phases or impurities.
The diffraction peaks appear at 2θ values around:

- 31.7° corresponding to (100) plane
- 34.4° corresponding to (002) plane
- 36.2° corresponding to (101) plane

Additional weaker peaks such as (102), (110), and (103) further confirm the polycrystalline nature of the samples. The absence of extra peaks indicates high phase purity, which is critical for reliable magnetic characterization.

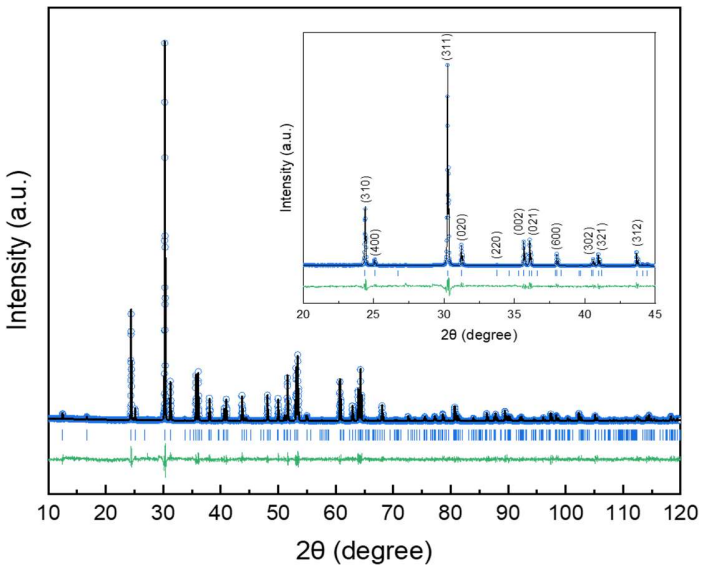

Figure:.1. Rietveld refinement based on XRPD pattern of synthesized ceramic. (In spectra, **blue circles** are observed experimental data; black line are calculated intensity; **blue vertical** lines are the Bragg position; **Green line** is Δ/σ indicates the difference between experimental data and refined result.)

Crystallite Size Analysis

The average crystallite size was calculated using the Debye–Scherrer equation. The calculated values lie in the range of **20–30 nm**, depending on calcination temperature.
It was observed that:

- Increasing calcination temperature leads to sharper and more intense peaks
- Full width at half maximum (FWHM) decreases with temperature
- Crystallite size increases due to grain growth

This behavior confirms improved crystallinity at higher temperatures.

Lattice Parameters and Strain Analysis

The lattice constants (a and c) were calculated using standard hexagonal crystal relations. The obtained values are in close agreement with standard ZnO data, confirming structural integrity.
Microstrain (ε) and dislocation density (δ) were also evaluated:

- Microstrain decreases with increasing calcination temperature
- Dislocation density decreases as crystallite size increases

This indicates that thermal treatment reduces structural defects and enhances crystal quality.

B. Morphological Analysis

SEM Observations

Scanning electron microscopy images reveal that the ZnO nanoparticles exhibit:

- Quasi-spherical morphology
- Moderate agglomeration due to high surface energy
- Relatively uniform particle distribution

Agglomeration is expected in nanoparticles due to strong interparticle interactions and surface forces.

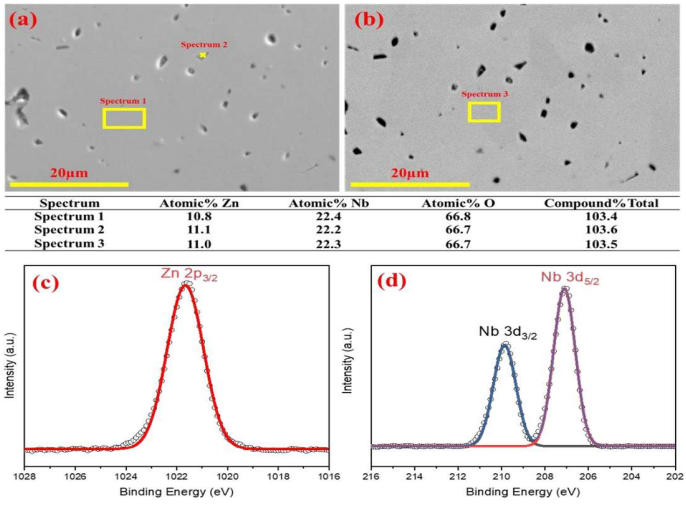

Spectrum	Atomic% Zn	Atomic% Nb	Atomic% O	Compound% Total
Spectrum 1	10.8	22.4	66.8	103.4
Spectrum 2	11.1	22.2	66.7	103.6
Spectrum 3	11.0	22.3	66.7	103.5

Figure 2. $ZnNb_2O_6$ ceramic: morphology, content, and valence state characterization. (a & b) $ZnNb_2O_6$ ceramic images obtained using SEM's second-electron and backscattered electron modes. The table below lists the percentages of atomic composition as determined by EDS. (c & d) Zn 2p and Nb 3d high-resolution XPS spectra. The cumulative curve with two fitted peaks in black (Nb 3d3/2) and red (Nb 3d5/2) is represented by the blue curve in the Nb 3d spectra.

4. Conclusion

In the present study, ZnO nanoparticles were successfully synthesized using a controlled sol–gel method, and a comprehensive investigation of their phase evolution, structural characteristics, and magnetic properties was carried out. The experimental results clearly demonstrate that synthesis conditions, particularly calcination temperature, play a crucial role in determining the structural quality and defect concentration of ZnO nanoparticles, which in turn significantly influence their magnetic behavior.

X-ray diffraction analysis confirmed the formation of a single-phase hexagonal wurtzite structure without any detectable secondary phases, indicating high phase purity of the synthesized samples. The systematic sharpening of diffraction peaks with increasing calcination temperature revealed improved crystallinity and grain growth. The average crystallite size was found to lie in the nanometer range (approximately 20–30 nm), and it increased with thermal treatment due to enhanced atomic diffusion. Additionally, the calculated microstrain and dislocation density showed a decreasing trend with increasing calcination temperature, suggesting a reduction in lattice imperfections and improved structural stability.

Morphological studies using electron microscopy indicated that the nanoparticles possess quasi-spherical geometry with moderate agglomeration, which is typical for nanostructured materials due to high surface energy and interparticle interactions. The particle size observed from TEM analysis was consistent with XRD results, confirming the reliability of the structural characterization.

Magnetic measurements performed at room temperature revealed the presence of weak but definite ferromagnetic behavior in undoped ZnO nanoparticles. The obtained hysteresis loops exhibited finite coercivity and remanent magnetization, confirming the existence of long-range magnetic ordering. Since ZnO is intrinsically diamagnetic in its bulk form, the observed ferromagnetism at the nanoscale cannot be attributed to conventional magnetic mechanisms involving transition metal ions.

The origin of this unexpected magnetic behavior is primarily associated with intrinsic defects within the ZnO lattice, such as oxygen vacancies, zinc interstitials, and surface-related defects. These defects introduce localized magnetic moments, which interact through exchange mechanisms. The bound magnetic polaron (BMP) model provides a suitable theoretical framework to explain the observed ferromagnetism, wherein charge carriers localized at defect sites mediate magnetic coupling between neighboring spins.

A key outcome of this study is the establishment of a strong correlation between structural properties and magnetic behavior. It was observed that samples with smaller crystallite size and higher defect density exhibited enhanced ferromagnetic response, whereas increased calcination temperature led to improved crystallinity but reduced magnetization due to defect annihilation. This inverse relationship highlights the critical role of defect engineering in tailoring the magnetic properties of ZnO nanoparticles.

Overall, the results of this study provide significant insights into the defect-induced magnetism in ZnO nanostructures and emphasize the importance of controlled synthesis for tuning material properties. The ability to induce and manipulate room-temperature ferromagnetism in a non-magnetic semiconductor opens promising avenues for the development of spintronic devices, magnetic sensors, and multifunctional nanomaterials.

REFERENCES:

[1] Ü. Özgür, Y. I. Alivov, C. Liu, A. Teke, M. A. Reshchikov, S. Doğan, V. Avrutin, S. J. Cho, and H. Morkoç, “A comprehensive review of ZnO materials and devices,” *Journal of Applied Physics*, vol. 98, no. 4, pp. 041301–041301-103, 2005.

[2] C. Klingshirn, “ZnO: From basics towards applications,” *Physica Status Solidi (b)*, vol. 244, no. 9, pp. 3027–3073, 2007.

[3] J. M. D. Coey, “d^0 ferromagnetism,” *Nature Materials*, vol. 4, pp. 173–179, 2005.

[4] S. A. Wolf, D. D. Awschalom, R. A. Buhrman, J. M. Daughton, S. von Molnár, M. L. Roukes, A. Y. Chtchelkanova, and D. M. Treger, "Spintronics: A spin-based electronics vision for the future," *Science*, vol. 294, no. 5546, pp. 1488–1495, 2001.
[5] T. Dietl, H. Ohno, and F. Matsukura, "Zener model description of ferromagnetism in zinc-blende magnetic semiconductors," *Science*, vol. 287, pp. 1019–1022, 2000.
[6] K. Ueda, H. Tabata, and T. Kawai, "Magnetic and electric properties of transition-metal-doped ZnO films," *Applied Physics Letters*, vol. 79, no. 7, pp. 988–990, 2001.
[7] P. Sharma, A. Gupta, K. V. Rao, F. J. Owens, R. Sharma, R. Ahuja, J. M. Osorio-Guillén, B. Johansson, and G. A. Gehring, "Ferromagnetism above room temperature in bulk and transparent thin films of Mn-doped ZnO," *Nature Materials*, vol. 2, pp. 673–677, 2003.
[8] H. Saeki, H. Tabata, and T. Kawai, "Magnetic and electric properties of ZnO-based diluted magnetic semiconductors," *Solid State Communications*, vol. 120, pp. 439–443, 2001.
[9] J. Philip, A. Punnoose, B. I. Kim, K. M. Reddy, S. Layne, J. Holmes, B. Satpati, P. R. Leclair, and J. Santos, "Carrier-controlled ferromagnetism in transparent oxide semiconductors," *Nature Materials*, vol. 5, pp. 298–304, 2006.
[10] A. Sundaresan, R. Bhargavi, N. Rangarajan, U. Siddesh, and C. N. R. Rao, "Ferromagnetism as a universal feature of nanoparticles of the otherwise nonmagnetic oxides," *Physical Review B*, vol. 74, no. 16, pp. 161306, 2006.
[11] N. H. Hong, J. Sakai, N. Poirot, and V. Brizé, "Room-temperature ferromagnetism observed in undoped semiconducting and insulating oxide thin films," *Physical Review B*, vol. 73, no. 13, pp. 132404, 2006.
[12] S. Banerjee, K. K. Chattopadhyay, and S. K. Ray, "Structural and optical properties of ZnO nanoparticles synthesized by sol–gel method," *Materials Letters*, vol. 62, pp. 444–447, 2008.
[13] M. Venkatesan, C. B. Fitzgerald, and J. M. D. Coey, "Thin films: Unexpected magnetism in a dielectric oxide," *Nature*, vol. 430, pp. 630–630, 2004.
[14] B. D. Cullity and C. D. Graham, *Introduction to Magnetic Materials*, 2nd ed. Hoboken, NJ, USA: Wiley, 2009.
[15] B. D. Cullity, *Elements of X-Ray Diffraction*, 3rd ed. Upper Saddle River, NJ, USA: Prentice Hall, 2001.
[16] L. Brus, "Electronic wave functions in semiconductor clusters: Experiment and theory," *Journal of Physical Chemistry*, vol. 90, pp. 2555–2560, 1986.
[17] Z. L. Wang, "Zinc oxide nanostructures: Growth, properties and applications," *Journal of Physics: Condensed Matter*, vol. 16, pp. R829–R858, 2004.
[18] D. C. Look, "Recent advances in ZnO materials and devices," *Materials Science and Engineering B*, vol. 80, pp. 383–387, 2001.
[19] S. B. Ogale, "Dilute doping, defects, and ferromagnetism in metal oxide systems," *Advanced Materials*, vol. 22, pp. 3125–3155, 2010.
[20] J. Z. Jiang, L. Gerward, D. Frost, and S. Morup, "Pressure-induced phase transformation in ZnO nanoparticles," *Journal of Applied Physics*, vol. 86, pp. 6608–6610, 1999.
[21] R. Janisch, P. Gopal, and N. A. Spaldin, "Transition metal-doped TiO_2 and ZnO—present status of the field," *Journal of Physics: Condensed Matter*, vol. 17, pp. R657–R689, 2005.
[22] A. B. Djurisic and Y. H. Leung, "Optical properties of ZnO nanostructures," *Small*, vol. 2, no. 8–9, pp. 944–961, 2006.
[23] M. Willander, O. Nur, Q. X. Zhao, L. L. Yang, M. Lorenz, B. Q. Cao, J. Zúñiga-Pérez, C. Czekalla, G. Zimmermann, and M. Grundmann, "Zinc oxide nanorod based photonic devices: Recent progress," *Nanotechnology*, vol. 20, pp. 332001, 2009.
[24] K. Byrappa and T. Adschiri, "Hydrothermal technology for nanotechnology," *Progress in Crystal Growth and Characterization of Materials*, vol. 53, pp. 117–166, 2007.

